Award No. DE-SC0013830

Issued by Department of Energy

YBCO Coated Conductor with an Integrated Optical Fiber Sensor

Final Report

March 31, 2016

Prepared by

Srivatsan Sathyamurthy and Martin Rupich

American Superconductor Corporation

Devens, MA 01434

And

Justin Schwartz

North Carolina State University

Raleigh, NC 27695

Table of Contents

Executive Summary

A proof-of-principle of the concept of integrating an optical fiber sensor with the lamination process used for 2G wires was successfully demonstrated. Taking advantage of one of the unique features of AMSC's 2G wires, namely the solder fillets, this concept provides the opportunity to incorporate an optical fiber sensor in intimate contact with the wire for the entire length of the conductor thus proving continuous sensing along the length. The Phase I work focused on (i) identifying appropriate optical fiber compatible with the 2G wire architecture and the lamination process, (ii) integrating the optical fiber sensor into the 2G wire architecture, (iii) evaluating the electrical and mechanical properties of the fiber-integrated 2G wire, (iv) evaluating the optical properties of the fiber after integration into the wire by lamination, (v) testing the quench detection capability of the fibers integrated into the 2G wire.

The major accomplishments of the Phase I program were:

- Proof-of-Principle demonstration of the concept of fiber integration into AMSC 2G wire
- Evaluation of electrical and mechanical properties of the fiber integrated wire
- Demonstration of superior quench detection capability of the optical fibers integrated into the 2G wire

The successful demonstration of the concept of fiber integration and the superior quench detection capabilities provided by the integrated optical fiber sensor together provide a means to fabricate a self-monitoring 2G-wire. Such self-monitoring 2G wires would provide a significant advantage when used in a high field superconducting magnet by providing a more robust means for quench detection and protection. The successful results in the Phase I program support the need to scale-up this process for manufacturing longer lengths of this self-monitoring wire for larger coil demonstrations as is proposed in the Phase II program.

Introduction and Overview

Project Objectives

The overall objectives of this Phase I project was to develop a manufacturing approach for incorporating optical fibers into the solder fillets of AMSC coated conductors and demonstrate their efficacy as a strain monitor and quench detection sensor.

The primary technical objectives of the Phase I project include

1 – Identification of optical fiber compatible with AMSC 2G-HTS wire

2 – Establish technical feasibility of embedding an optical fiber within the Solder fillet of AMSC's 2G-coil wire

3 – Characterize the strain sensitivity and responsiveness of the embedded optical fibers

4 – Fabricate long lengths of self-monitoring 2G coil wire

5 – Demonstrate the ability to detect a quench condition in a coil produced with a self-monitoring 2G wire

Technical Approach

Understanding the quench behavior of high field superconducting magnets is an absolute necessity for safe operation. The current quench behavior understanding is based on LTS-magnets. While the basic physics of quench for HTS-magnets is similar, there are significant qualitative differences. The aim of a quench protection system is to avoid a permanent degradation of the conductor properties in the event of a fault that induces a quench. Any quench protection system involves: (1) detection of a hot-spot, (2) assessment to determine if the hot-spot will lead to a quench and (3) preventive action should the magnet go through a quench. In case of HTS-magnets, due to the very slow Normal Zone Propagation Velocity, the biggest challenge is quench detection. So any technology that facilitates early quench detection, significantly improves the effectiveness of the quench protection system.

Over the last few years, optical fiber sensors have evolved to meet a number of sensing needs, using a variety of interrogation techniques. For the purposes of quench detection, optical fibers show a spectral shift as a response to local temperature changes, and with an appropriate interrogator, this spectral shift can be utilized to detect a hot-spot or disturbance which may lead to a quench. This approach makes it possible to detect a potential quench more quickly than the conventional voltage signal measurements.

One of the main challenges facing the use of optical fibers for quench detection is ensuring uniform, intimate contact between the fiber and the conductor along the entire length of the conductor. The unique advantage offered by the AMSC Amperium wire where the solder fillets formed during

lamination run the whole length of the wire, and can accommodate an optical fiber, provides a means to maintain intimate contact between the fiber and the conductor. Such a fiber integrated wire with intimate contact extending along the entire length of the conductor could provide a means for continuous sensing without any decrease in engineering current density or winding pack current density of the magnet, thus resulting in a self-monitoring conductor.

During Phase I, AMSC focused on identifying the proper optical fiber and coatings that will be conducive to handling and compatible with the solder and wire dimensions. Once the appropriate fiber was identified, short lengths of composite wire integrated with the optical fiber were fabricated using a static process in the AMSC splice apparatus. To keep the approach simple and inexpensive, commercially available fibers with two different diameters (50µm and 80µm), and different surface coatings (polymer, Au, Ag) on the fiber were tested for ease of handling. The mechanical properties of the fiber embedded samples were tested to establish whether the presence of the fiber alters the mechanical properties of the wire.

After establishing the mechanical properties of the short length samples, fiber embedded wires in longer lengths (>30cm) were prepared. Due to the time constraints and budget limitations of the Phase I project, these samples were prepared in a static process using the same splice apparatus. These fiber embedded samples were further evaluated at NCSU. The embedded fibers were first interrogated at room temperature to ensure that they survived the manufacturing process. This was followed by an evaluation of the fibers at 77K to ensure that the fibers can survive the differential thermal contraction between the solder and fiber. Following these initial tests, NCSU carried out mechanical and quench testing of these samples.

The results obtained from the various experiments are summarized under the various proposed tasks below.

Phase I Results

Task 1: Optical Fiber Selection

NCSU evaluated commercial optical fibers for their suitability for quench detection and their compatibility with the AMSC 2G wire process. The wettability and the ease of handling were evaluated for fibers with dual-acrylate or polyamide coatings and ones with the coating removed. Also tested were fibers with an Au-Pd or Ag coating to check for improved wetting by solder.

The following commercially available optical fibers were acquired and considered for being embedded into the solder fillet of AMSC Amperium wires:

- Nufern PM1550G-40/90-5, which is a single mode fiber with a cladding size of 40 µm and a dual-acrylate coating of 50 µm in thickness (Nufern 40/90).
- Thorlabs SM1500G80, which is a single mode fiber, with a 80 µm cladding with a dual-acrylate coating of 170 µm in diameter (Thorlabs 80/170).
- Luna 80 µm cladding diameter with a 10 µm thick polyamide coating (Luna 80/100).

Different coating materials and techniques have been explored and evaluated prior to the lamination of the fiber into the AMSC wire, to ensure that the fiber was compatible with the solder used by AMSC in the fillet and with the lamination process. The compatibility with the lamination process requires that the fiber be strong enough to survive the process without breaking. The other requirement is that the fiber allows for an adequate lamination process that provides good bonding between the HTS, copper strips and optical fiber.

The first approach followed was to remove the additional coating that is standard on all commercial optical fibers (typically, as well as in our cases, either dual-acrylate or polyamide). Both are polymeric coatings applied to the cladding surface. The functions of the coating layer are primarily to provide ductility and to protect the glass cladding from chemical and mechanical perturbations. Furthermore, a metallic coating should bond better to silica (cladding) than to acrylate. The dual acrylate coating has been removed by simply burning it off with a flame. In figure 1, a cross section of the Luna 80/100 optical fiber coated with a thin layer of Au-Pd is shown. The dual acrylate coating of the Thorlabs 80/170 was removed, mainly to meet the size requirement that comes with embedding the fiber into the solder fillet of AMSC wires. The resulting fiber, which consists of only 80 µm diameter silica cladding, was very fragile when it was mounted to be sputter coated. Another coating method that has been considered is pulsed laser deposition (PLD), but once the bare fiber (without polymeric coating) was mounted onto a sample stage for deposition, it broke multiple times, showing itself to be too fragile for surviving the coating process as well as the lamination into AMSC wires.

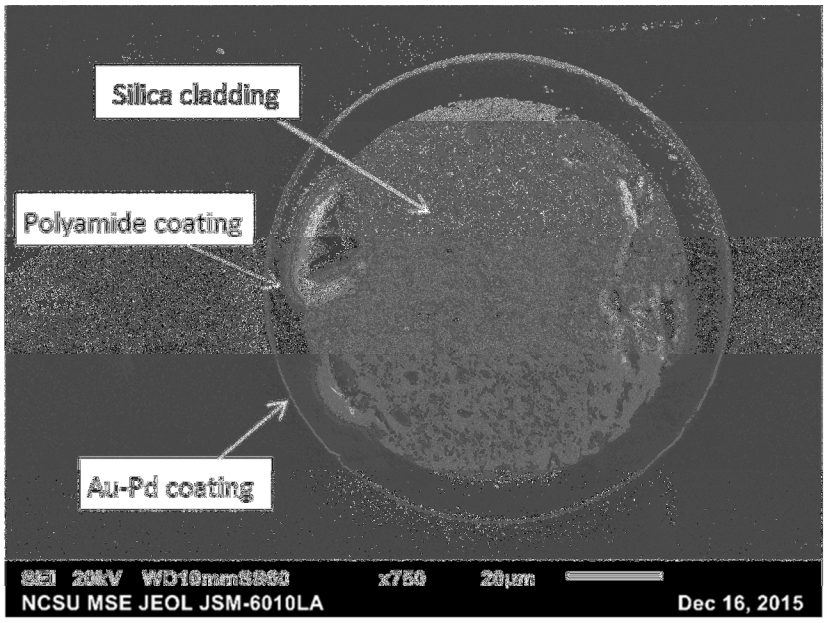

Figure 1 – SEM secondary electrons micrograph of a cross section of the Luna 80/10 optical fiber

Analogous results have been obtained using the Nufern 40/90, which is also too fragile in its bare condition (without polymeric coating) to withstand a possible metallic coating via either sputtering or PLD and, most importantly, to withstand the lamination process, especially in view of the continuous reel to reel lamination process that will need to be used to achieve longer length of smart wires in phase

II. Since the polymeric coating showed to be necessary to retain ductility and allow the optical fiber to survive intact the lamination process, the Luna fiber with a 80 µm cladding and a 10 µm polyamide coating has been chosen for the lamination process. Although the deposition of a metallic coating on top of the polyamide is viable (showed in figure 1 is a Au-Pd coating deposited onto the polyamide via plasma sputtering) the embedding of the commercially available polyamide coated fiber has been addressed first and with success.

Through these tests it was determined that optical fibers were too brittle and incompatible with the AMSC 2G wire process when the polymeric coating was removed. While the addition of metal coating helps wettability by solder, it may not be necessary for the incorporation of the fiber into the 2G wire.

Task 2: Optical Fiber Incorporation into 2G Coil wire

Based on the work performed under Task 1, it was clear that both coated and uncoated fibers may be suitable for incorporation into the laminated wire. The fibers were incorporated into short lengths of wires (10-20cm) in the fillet using a 12mm copper laminated coil wire. This was carried out using a modified splicing system available at AMSC (see Figure 2). This system is capable of laminating ~10 cm of wire at a time. This was adapted to laminate longer lengths by overlapping shorter segments of assembled lamina and insert in the lamination zone.

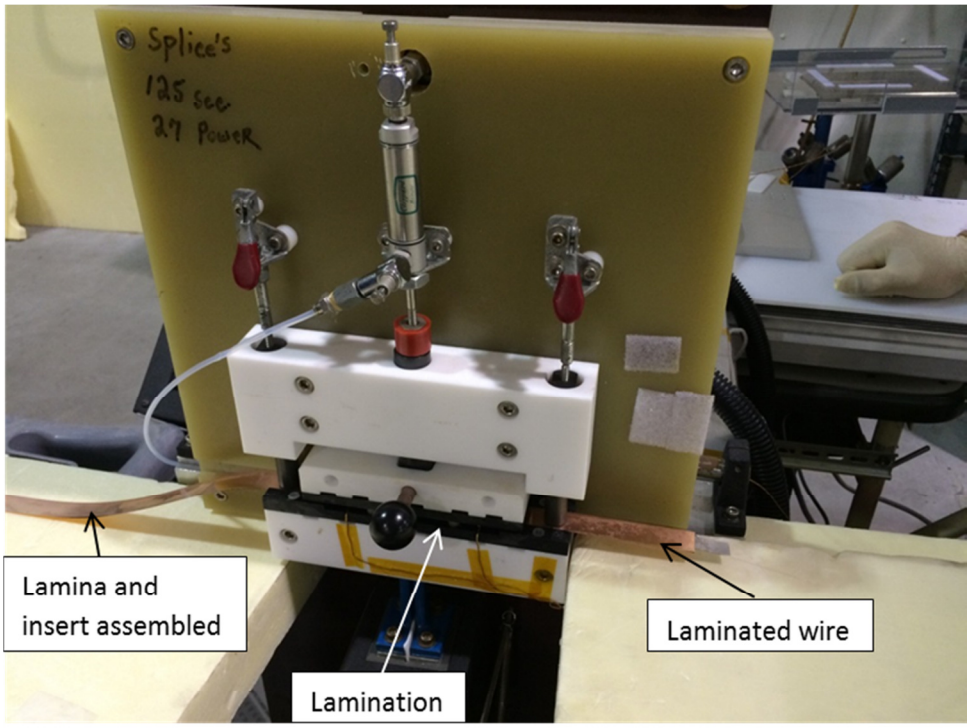

Figure 2 – Static lamination apparatus at AMSC

Multiple solders were assessed for this purpose, and it was concluded that lower melting solders based on In alloys were better suited for this purpose when using the static soldering set up. The fiber integrated samples were mounted and polished for cross-section microscopy. Figure 3 (a) and (b) shows

the back-scattered image of the insert-lamina along with the solder fillet, and the fiber incorporated in the fillet. The cracks observed at the fiber surface could be attributed to the sample handling during mounting and polishing of these samples. In addition to the cracks, there is a significant amount of porosity observed in the solder fillet near the fiber. Such porosity in the fillet could influence the mechanical properties of the wire.

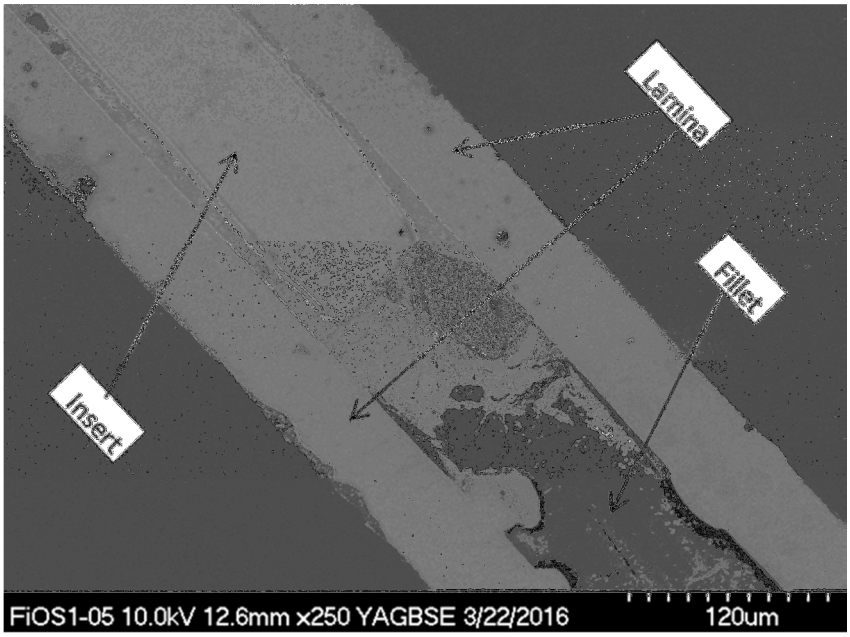

Figure 3a – SEM micrograph showing a cross section of the smart conductor in the region across the HTS insert and the solder fillet

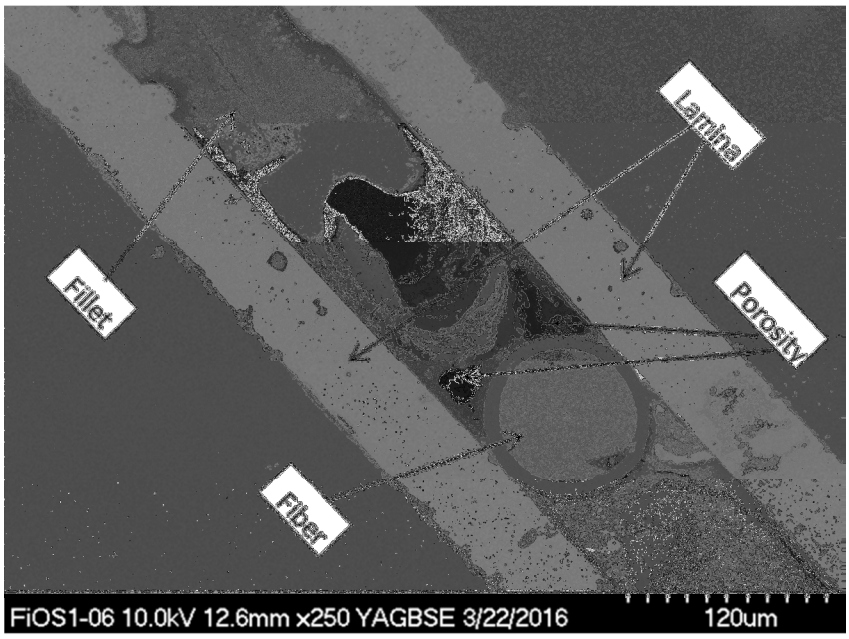

Figure 3b – SEM micrograph showing a cross section of the smart conductor that includes the region of the fillet where the optical fiber is embedded

Figure 4 shows a higher magnification image of the fiber interface with the fillet and the lamina. Inspite of the porosity, these images show a good wetting of the fiber by the solder. This suggests that even with the polyamide coating, the fibers do not tend to dewet from the solder in the fillet. Also, the polyamide coating (the annular region surrounding the fiber in the images) seems to be intact after the soldering process. This suggests that the polyamide coating can withstand the low temperature soldering process being used. The presence of this polyamide coating intact around the fiber should significantly aid maintaining the mechanical integrity of the fiber during sample handling as well as increase the sensitivity to thermal disturbances, due to the higher coefficient of thermal expansion than silica.

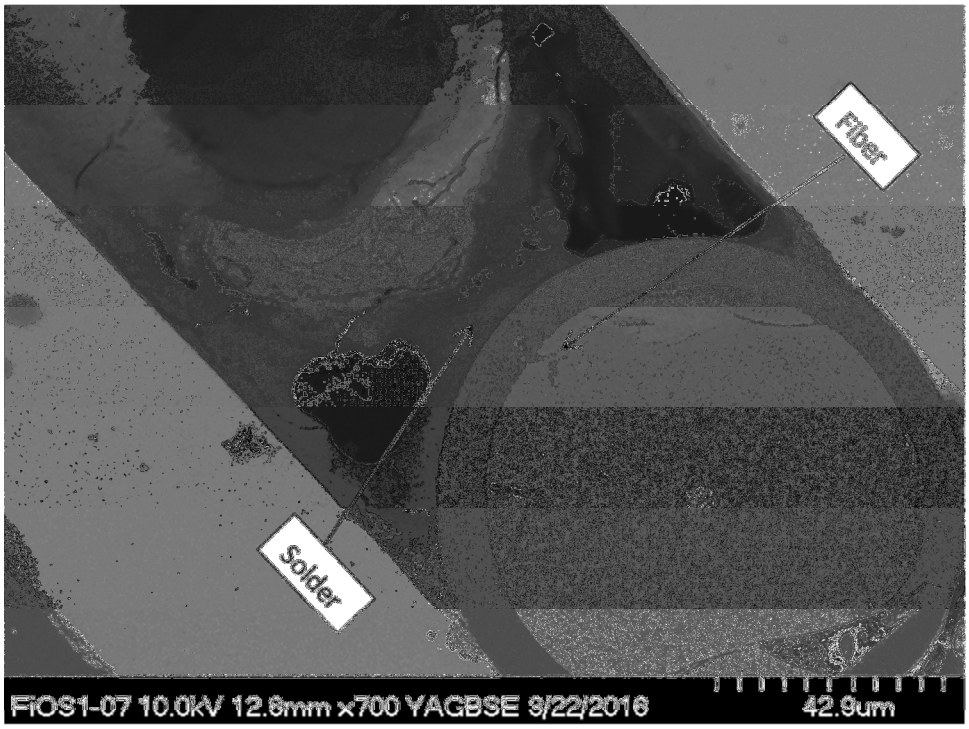

Figure 4 - SEM micrograph showing a cross section of the smart conductor with focus on the embedded optical fiber

For an optical fiber to be interrogated by Rayleigh scattering, it needs to be equipped with a connection and a termination. The connection simply allows the fiber to be connected to the optical interrogator that injects lights into the optical path and detects the backscattered signal. The termination is needed to minimize the signal reflected at the interface between the end of the fiber and the environment. All smart conductor samples manufactured included 15-20 cm of optical fiber extending out of both ends of the conductor (see figure 5). This allowed for mounting the connections and terminations. Since the 80 µm cladding fiber is too fragile to be spliced to connection and termination successfully, two segments of 125 µm cladding fiber were spliced to both ends of the 80 µm fiber and then to the connector and

termination. Figure 6 depicts a schematic that illustrates the splicing pattern and includes pictures of the splices.

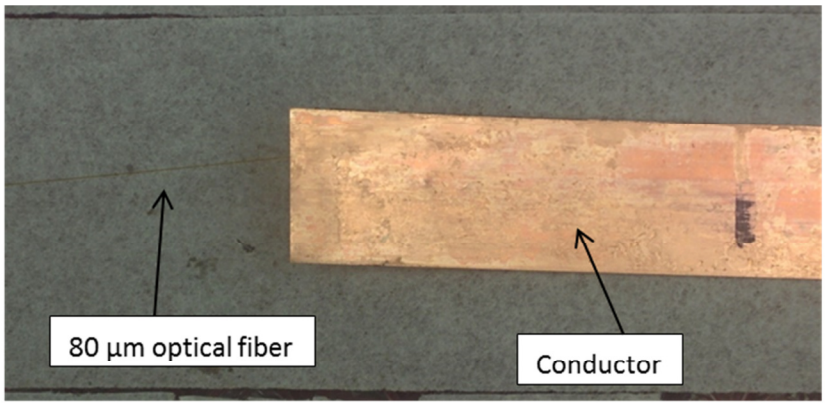

Figure 5 – Image of the smart wire that highlights the optical fiber extending out of the conductor end. The other end of the conductor is analogous.

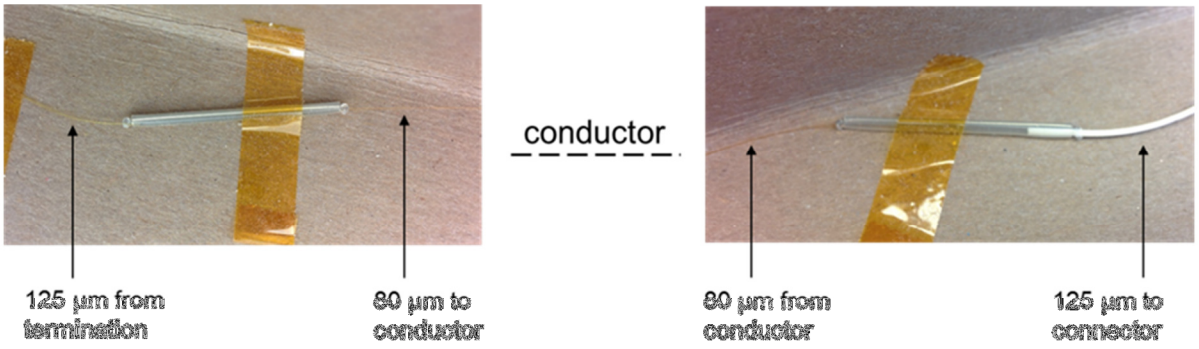

Figure 6 – Schematic illustrating the splicing pattern and the use of the 125 µm fiber to reach connection and termination. Read from left to right to go from termination to connection.

Task 3: Evaluating the strain-sensor capabilities of the self-monitoring 2G HTS wire

One of the 30 cm samples of smart conductor was mounted on a tensile test machine and subject to loads up to 50 lbs. Both the conductor itself and the optical fiber embedded in the conductor fully survived the tests, showing a robustness against tensile loads up to 50 lbs. The smart conductor clamped to the tensile test apparatus is shown in figure 7. With the conductor clamped to the tensile test machine, the optical fiber coming out of the smart conductor was connected to the optical interrogator to measure the spectral shift during testing. The test consisted in increasing the load linearly with a ramp rate of about 1.15 lbs/s. The test was repeated with different maximum loads of 23, 30 and 50 lbs. The results of the test with a 30 lbs final load are shown in figure 8. Here the spectral shift is measured as a function of position along the smart conductor. Note that the conductor length is 30 cm, and the clamped regions are about 1-2 cm each. This is accurately reflected in the measurement, as the spectral shift is zero outside of a ~27 cm region, which is the region of conductor that is loaded, being within the clamps. As can be inferred from the shape of the curves plotted in figure 8, the spectral shift is likely to

be proportional to the extension of the sample. Therefore, dividing the extension by the length of the tape (as a function of the position along the conductor), the strain is obtained.

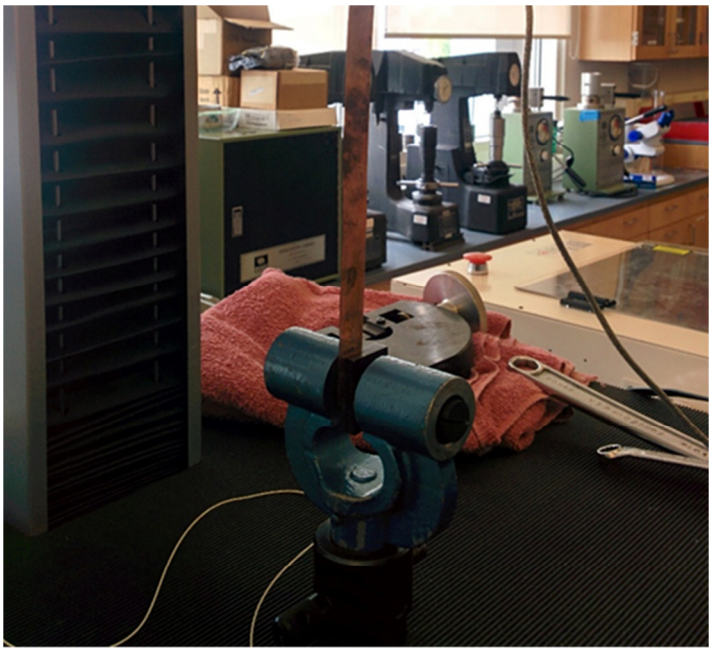

Figure 7 – Smart conductor clamped to tensile testing machine

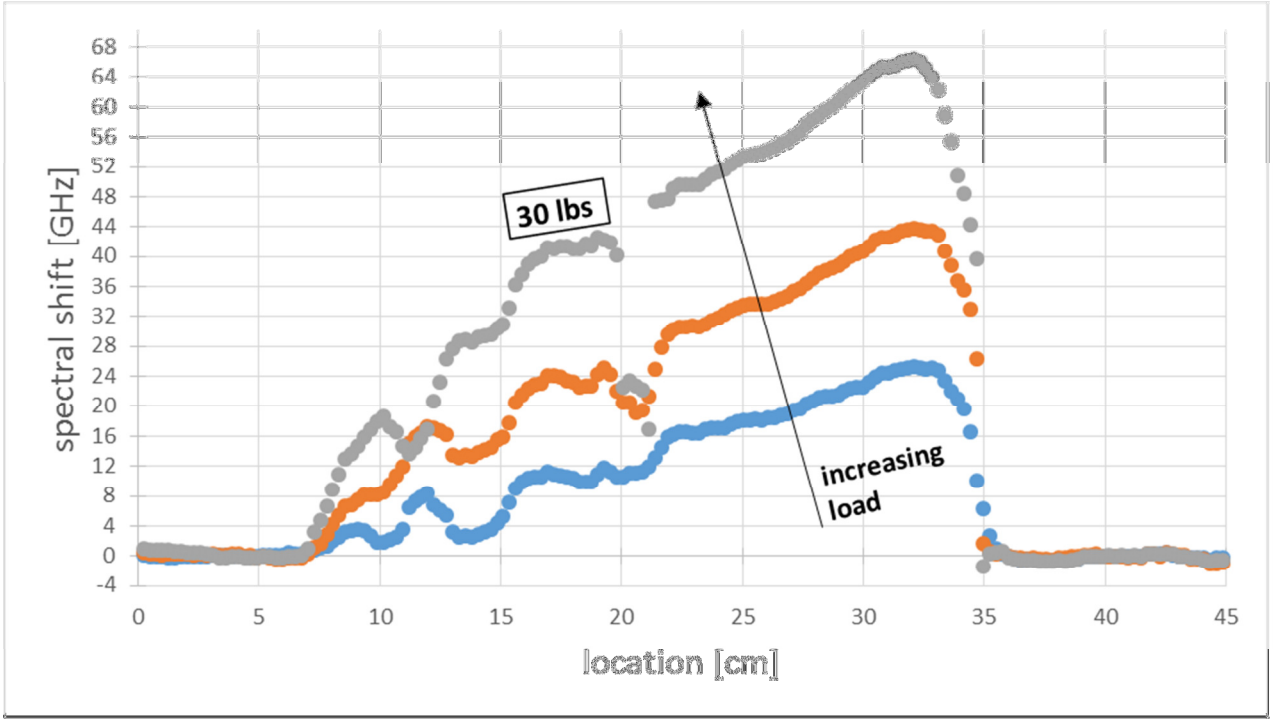

Figure 8 – Spectral shift measured during tensile test, as a function of positon along the conductor. The conductor is clamped to the tensile test machine at about 7 cm and 35 cm.

Since the spectral shift was proportional to the extension, dividing the spectral shift by the position a quantity proportional to the strain is obtained. This is shown in figure 9. The non-perfect linearity of the curves in figure 8 and 9 may be due to inhomogeneity in fiber bonding to the solder fillet matrix, which is consistent with the porosity observed in the solder fillet (see figures 3-4). The results for a maximum load of 23 lbs are shown in figure 10. An analogous plot was obtained for 50 lbs. The interpretation of the plot in figure 10 is analogous to that for figure 8. Figure 11 shows a summary of the 3 tests in terms of maximum spectral shift experienced during the tensile tests plotted against the maximum load of the test.

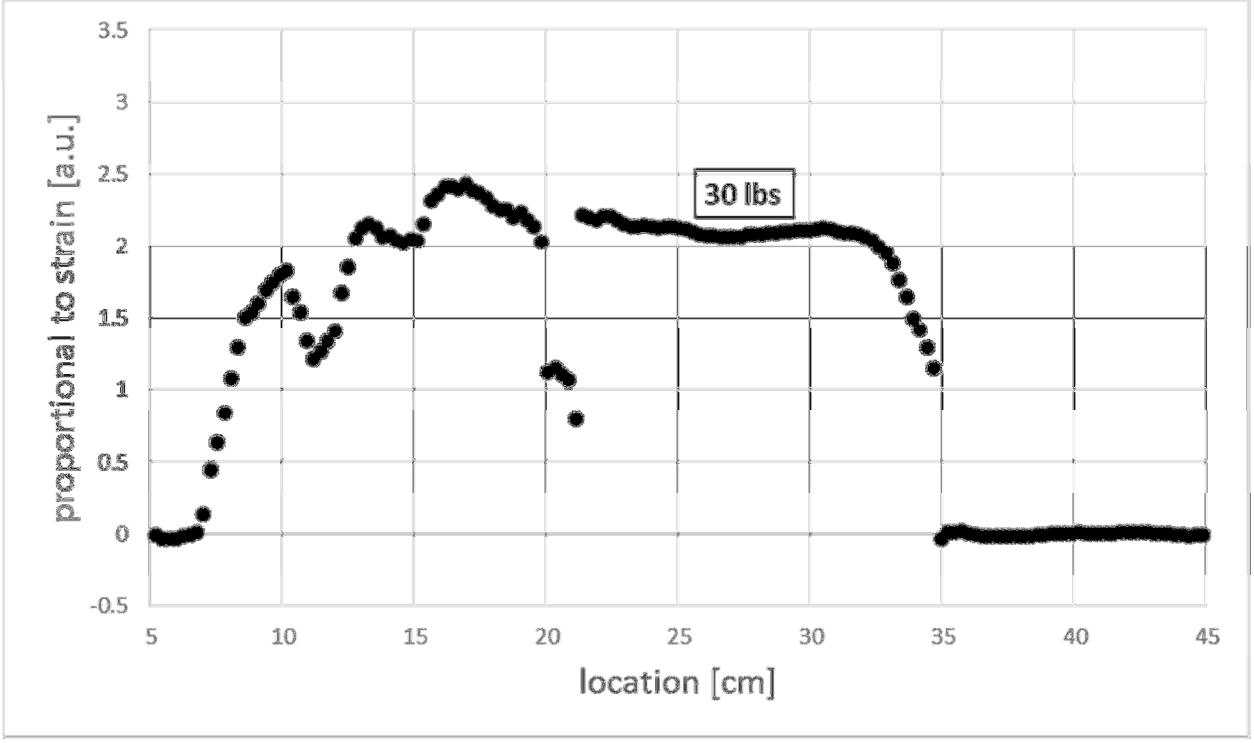

Figure 9 – Spectral shift divided by the position along the conductor, as a function of the position along the conductor. The conductor is clamped to the tensile test machine at about 7 cm and 35 cm.

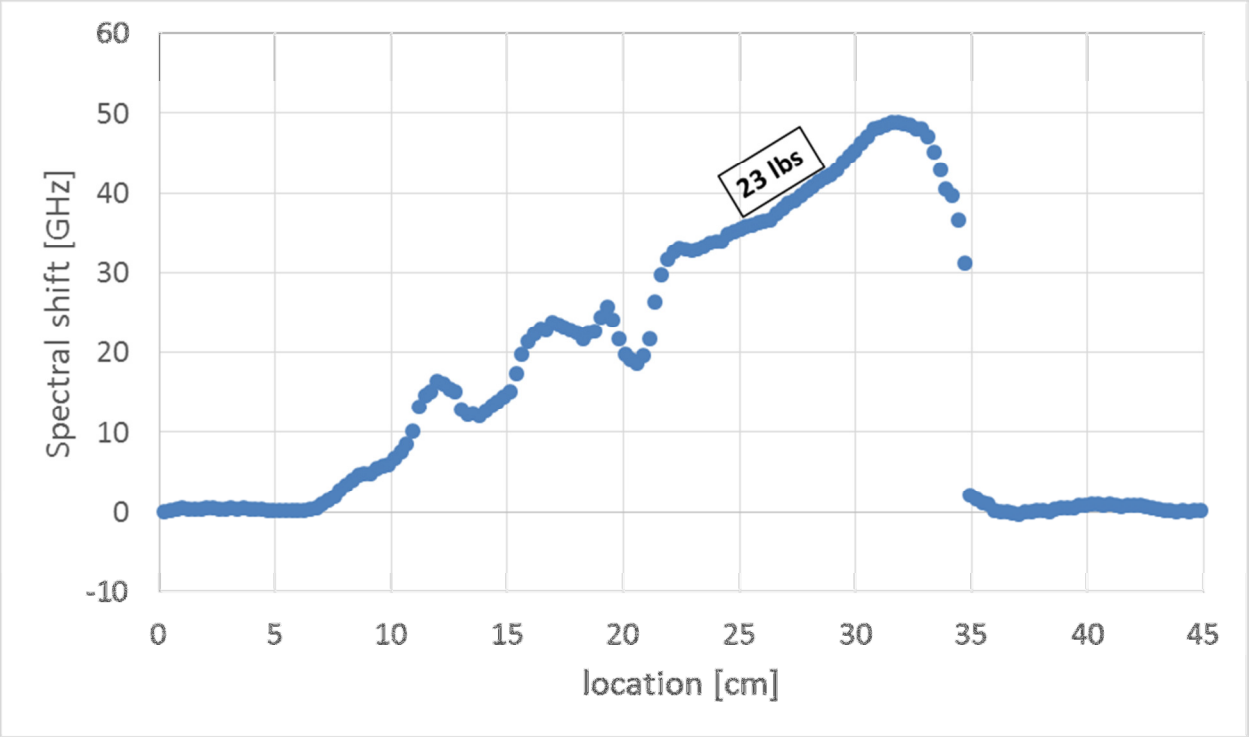

Figure 10 – Spectral shift measured during a tensile test at the maximum load of 23 lbs, as a function of position along the conductor.

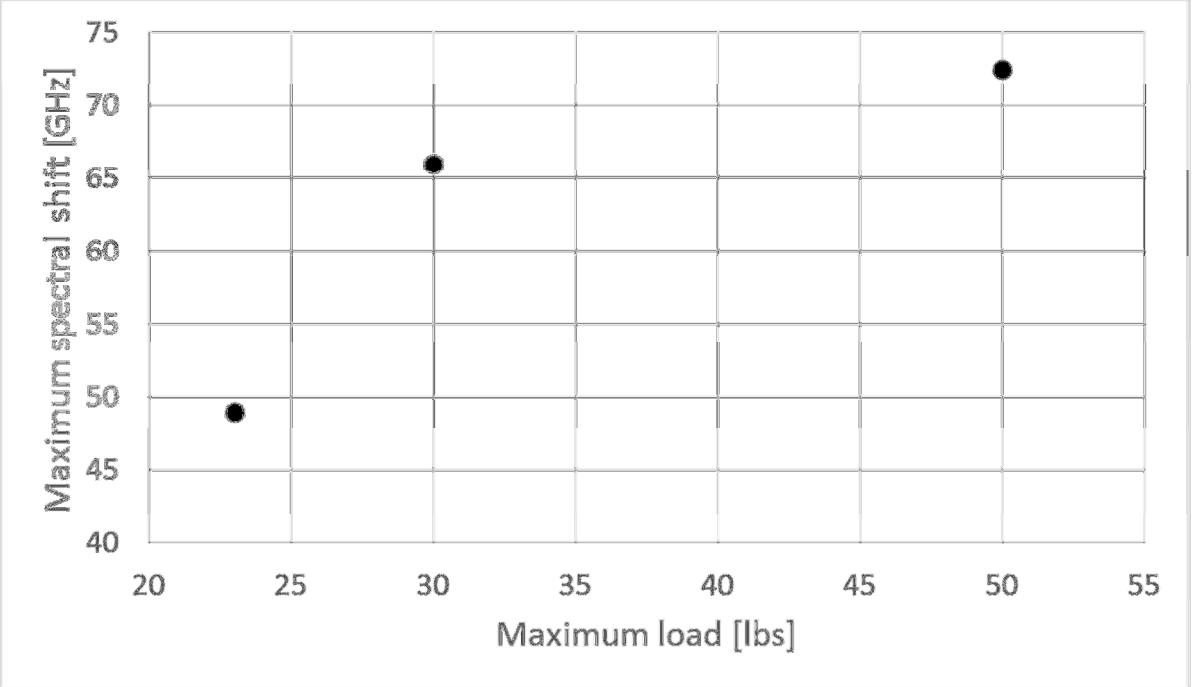

Figure 11 – Maximum spectral shift measured during tensile tests vs maximum load of the tensile test

Task 4: Manufacture 1-2 m length of self-monitoring 2G Coil wire

Using the approach developed in Task 2, longer lengths of the fiber integrated 2G coil wire were laminated. Although the ideal approach to incorporating the optical fiber in the composite wire is to use a reel-to-reel lamination line, the static approach was used similar to the one used in Task 2 to accommodate for the time and budget constraints associated with the Phase I project. The continuous reel-to-reel lamination will be part of Phase II.

The mechanical properties of these samples were subsequently tested. The solder fillets are an integral component of the wire and the mechanical properties of the wire are strongly influenced by the quality of these fillets. It is essential to understand how the presence of the fiber in the fillets affects mechanical properties. Of particular concern is the mismatch in thermal expansion of the fiber and the solder fillet having a detrimental effect on the mechanical properties of the wire. Three common mechanical tests performed on our standard wire, Double bend test, Stress Tolerance test, and Ic Strain were performed on these fiber integrated wires. The results from these tests are listed in Table 1, along with the requirements for the standard wires (without fiber integration). From these tests, it is clear that the performance of the fiber-integrated wire meets the requirements set for the standard wire. However, double bend test shows an increased drop in Ic than the 95% retention expected for the standard wire. This may be the limitation of the static lamination process, and is consistent with the porosity observed in the fillets (figures 3 and 4). Additionally, the critical current of the smart conductor was measured with a four-point probe method at 77 K, self-field, in liquid nitrogen. A conductor length of 20 cm was used, with voltage taps spaced 20 mm apart and centered on the conductor. The measurement yielded a critical current of 330 A and an n-value of 25.

Test	Fiber integrated wire performance	Standard wire requirements	
Double bend test	92% Ic retention	>95% Ic retention	
R.T. Stress Tolerance test	200MPa	>150MPa with 95% Ic retention	
Ic Strain test		0.404 % strain	0.3% strain with >95% Ic retention

Task 5: Quench testing of self-monitoring 2G coil wire

One of the 30 cm samples has been equipped with an embedded heater to generate a thermal disturbance, as well as conventional instrumentation like voltage taps and thermocouples. Figure 12 is an image illustrating the experimental setup. The test consists of cooling down the conductor to a temperature between 77 and 90 K, by means of nitrogen vapor. Once cooled, a heat pulse is released by the embedded heater while the spectral shift is measured.

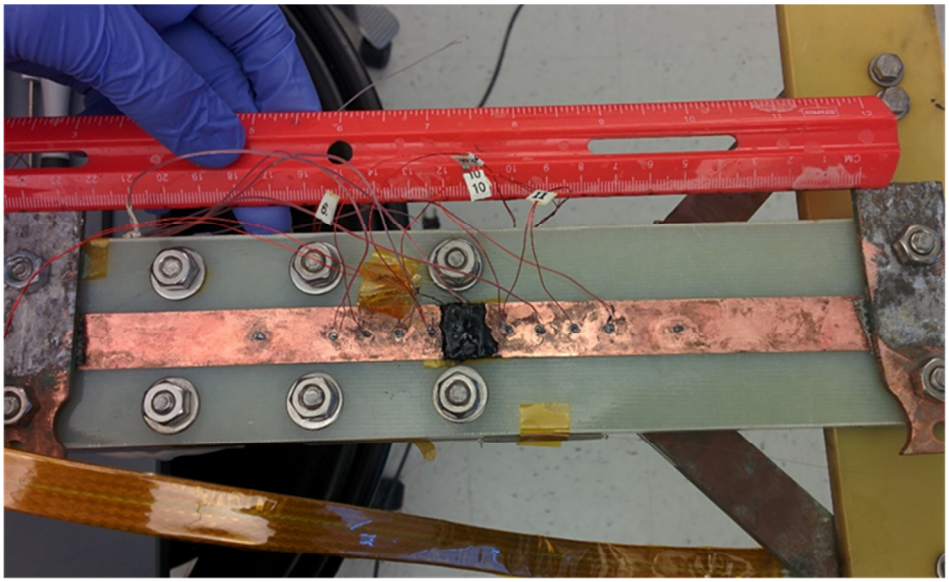

Figure 12 – Experimental setup for test of 30 cm conductor in nitrogen vapor. The black region is the heater embedded in stycast epoxy.

Figures 13-15 shows some of the results of one of these tests. The spectral shift increases right as the heat pulse occurred. Also to note is the low noise recorded during the test and the high signal to noise ratio of about 8. Figure 13 is a plot of the time evolution of the spectral shift during the test at an initial temperature of 79 K at the location of the heater whereas figure 14 shows the spatial behavior of the spectral shift during the same test. Note that the spatial resolution was 2.6 mm and the temporal resolution was 20 ms during these tests.

Prior to tests in the 79-90 K temperature range, analogous room temperature tests were performed and analogous results were obtained. Figure 15 shows a summary of two tests carried out at different temperatures; the graph plots the maximum spectral shift experienced in the conductor (maximum in space and time, therefore at the location of the heater and at the time when the maximum spectral shift occurred) vs the initial temperature (before the heat pulse) at the location of the heater. The heat released during the two tests is the same. At lower temperature, the lower specific heat results in a larger temperature change for the same heat release. This explains the higher signal at lower temperature. In a subsequent test, when a transport current was injected into the conductor, joule heating was detected by the spectral shift signal that occurred at the connections between current leads and conductor. This is due to the too high resistance of the current leads as well as poor electrical contact (the current leads were mechanically clamped to the conductor).

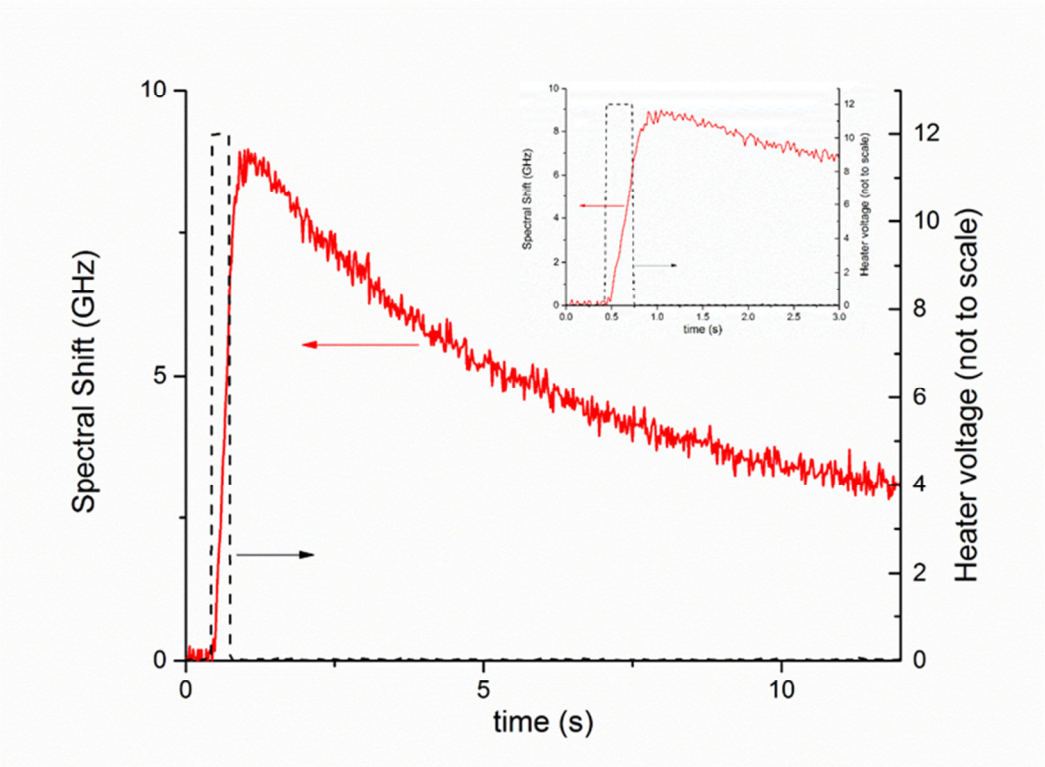

Figure 13 – Spectral shift measured at the position of its maximum as a function of time during a thermal disturbance at 79 K in Nitrogen vapor. The inset shows a higher magnification of the same plot to highlight the time evolution right after the heat pulse occurred.

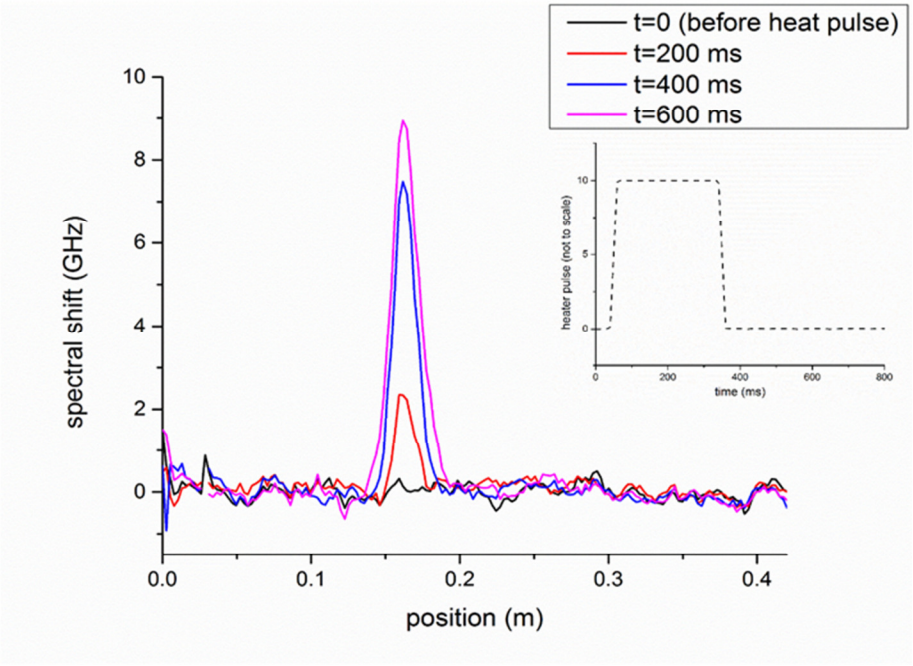

Figure 14 – Spectral shift as a function of position along the conductor at different times, before and after the heat pulse. Note that the conductor extends from about 0.02 m to about 0.32 m. The inset shows the heat pulse vs time.

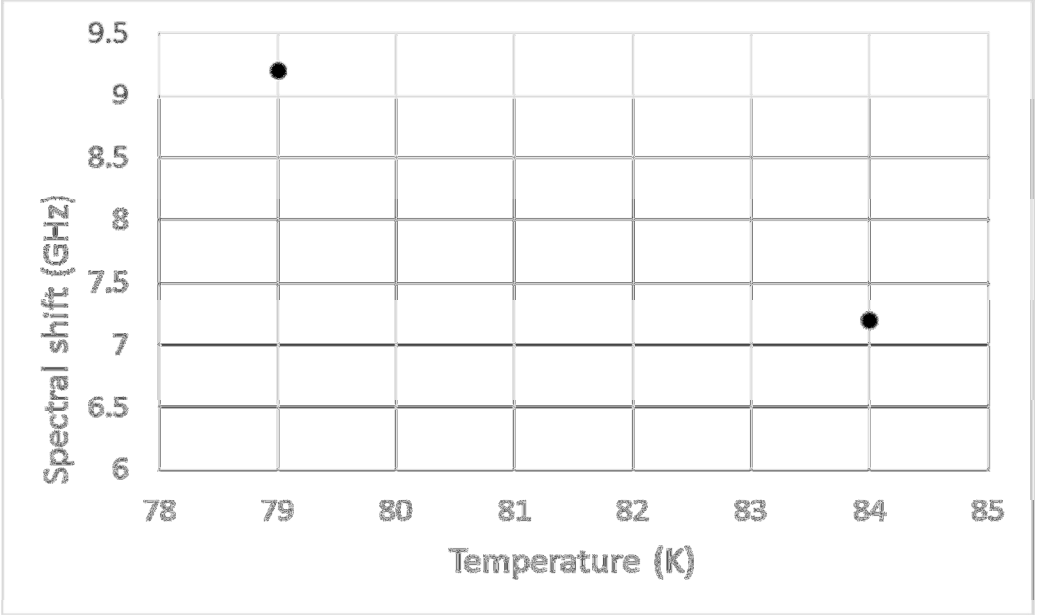

Figure 15 – Maximum spectral shift measured due to the same heat pulse, at different initial temperatures

Figure 16 shows an image of the connection between current leads and conductor and figure 17 shows the results of the test. Note that the distance between the clamps, which are the locations of the resistive heating, is exactly reflected in the spectral shift measurement to be about 22 cm (see figure 12 for comparison). Also, the reason of the different spectral shift increases at about 2.5 cm and 25 cm is due to the way the apparatus lies in the cryostat: the conductor is vertical in the cryostat, which implies that the lower connection to the current lead (at 25 cm in figure 17) is subject to stronger cooling than the upper connection (at 2.5 cm in figure 17), hence the stronger heating at upper current lead connection. In addition to these tests, all the smart conductors, including the 1 m long one, were interrogated to make sure that the optical fiber was intact and survived all the conductor manufacturing processes. All the manufactured smart conductors presented an intact optical fiber and were able to be interrogated by Rayleigh backscattering, generating the self-monitoring capabilities that were the central aim of this work.

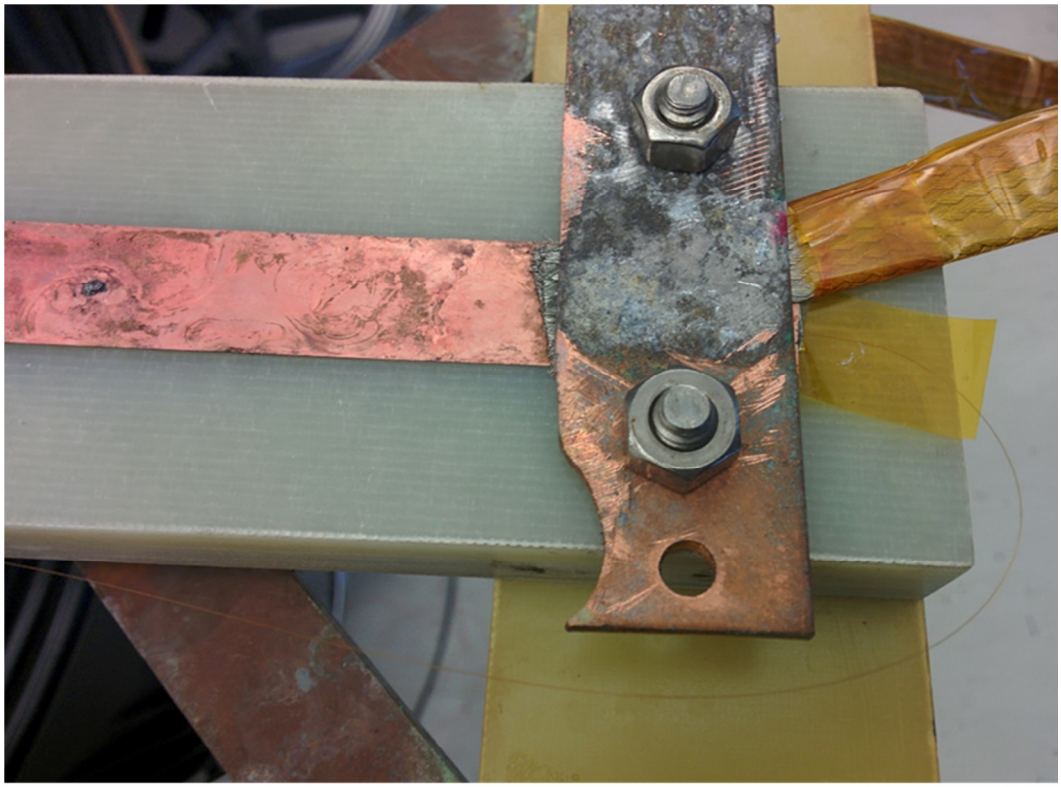

Figure 16 - – Image showing the connection between current lead and conductor

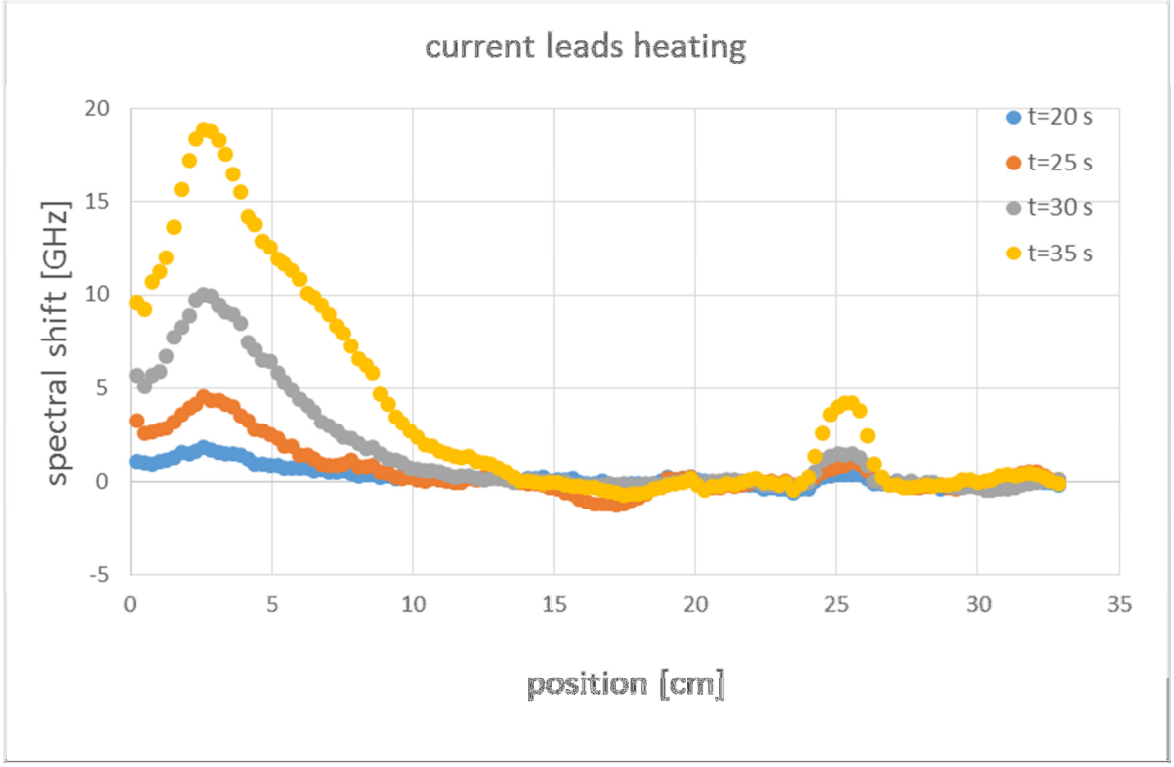

Figure 17 - Joule heating of the current leads detected by the spectral shift. The conductor is mechanically clamped to current leads

Summary

The primary objectives of the Phase I Project was to develop a proof-of-principle for a concept of integrating an optical fiber sensor into the laminated 2G wire, there by producing a functionalized 2G wire with self-monitoring capabilities. In this phase I work, we identified the appropriate commercially available fiber compatible with the laminated wire architecture, and with a polymer coating to ease handling during fabrication. Using a splicing apparatus, these fibers were integrated into the solder fillet of a 2G wire during lamination. The electrical, mechanical and optical properties of these fiber integrated wires were characterized, and the efficacy of the integrated optical fiber sensor in detecting temperature changes in the wire was evaluated.

The main accomplishments in this Phase I project include:

- Identification of an appropriate optical fiber compatible with the lamination process
- Integration of an optical fiber into the solder fillet during lamination
- Fabrication of ~30cm long fiber-integrated 2G wires
- Evaluation of the electrical and mechanical properties of the fiber integrated 2G wire
- Quench detection by Interrogation of the optical fiber to detect small changes in temperature in the wire using spectral shifts.